

Muon anomalous magnetic dipole moment in the $\mu\nu$ SSM

Hai-Bin Zhang^{a,b*}, Chang-Xin Liu^{a,b†}, Jin-Lei Yang^{c,d‡}, Tai-Fu Feng^{a,b,e§}

^a*Department of Physics, Hebei University, Baoding, 071002, China*

^b*Key Laboratory of High-precision Computation and Application of Quantum Field Theory of Hebei Province, Baoding, 071002, China*

^c*CAS Key Laboratory of Theoretical Physics, Institute of Theoretical Physics, Chinese Academy of Sciences, Beijing 100190, China*

^d*School of Physical Sciences, University of Chinese Academy of Sciences, Beijing 100049, China*

^e*College of Physics, Chongqing University, Chongqing, 400044, China*

Abstract

Recently, the Muon g-2 experiment at Fermilab has measured the muon anomalous magnetic dipole moment (MDM), $a_\mu = (g_\mu - 2)/2$, which reported that the new experimental average increases the tension between experiment and the standard model (SM) prediction to 4.2σ . In this work, we reanalyse the muon anomalous MDM at two-loop level in the μ from ν Supersymmetric Standard Model ($\mu\nu$ SSM) combined with the updated experimental average. The $\mu\nu$ SSM can explain the current tension between the experimental measurement and the SM theoretical prediction for the muon anomalous MDM, constrained by the 125 GeV Higgs boson mass and decays, the rare decay $\bar{B} \rightarrow X_s \gamma$ and so on. We also investigate the anomalous MDM of the electron and tau lepton, $a_e = (g_e - 2)/2$ and $a_\tau = (g_\tau - 2)/2$, at two-loop level in the $\mu\nu$ SSM. In addition, the 125 GeV Higgs boson decays to a pair of charged leptons in the $\mu\nu$ SSM are also analysed.

PACS numbers:

Keywords: Supersymmetry, Magnetic dipole moment, Higgs boson decays

* Corresponding author.

hbzhang@hbu.edu.cn

† LIUchangxinZ@163.com

‡ JLYangJL@163.com

§ fengtf@hbu.edu.cn

I. INTRODUCTION

The anomalous magnetic dipole moment (MDM) of the muon, $a_\mu = (g_\mu - 2)/2$, recently has been measured by the Muon g-2 experiment at Fermilab [1–4], which reported that the result is 3.3 standard deviations (σ) greater than the standard model (SM) prediction based on its Run-1 data and is in agreement with the previous Brookhaven National Laboratory (BNL) E821 measurement [5]. Combined with previous E821 measurement, the new experimental average for the difference between the experimental measurement and the SM prediction [6] of a_μ is given by

$$\Delta a_\mu = a_\mu^{\text{exp}} - a_\mu^{\text{SM}} = (25.1 \pm 5.9) \times 10^{-10}, \quad (1)$$

which increases the tension between the experimental measurement and the SM theoretical prediction to 4.2σ . This result will further motivate the development of the SM extensions. There are tons of papers researched the muon anomalous MDM in the Refs. [7–92] and references therein. However, it is worth mentioning that the latest result obtained by the lattice QCD calculation [93] of the leading order hadronic vacuum polarization contribution to a_μ is larger than the former result, which can accommodate the discrepancy between the experiment and the SM prediction, hence the discrepancy needs further scrutiny.

In this work, we will analyse the muon anomalous MDM at two-loop level in the μ from ν Supersymmetric Standard Model ($\mu\nu$ SSM) [94–100], combined with the new experimental average. Through introducing three singlet right-handed neutrino superfields $\hat{\nu}_i^c$ ($i = 1, 2, 3$), the $\mu\nu$ SSM can solve the μ problem [101] of the minimal supersymmetric standard model (MSSM) [102–106], and can generate three tiny neutrino masses through TeV scale seesaw mechanism [95, 107–113].

The corresponding superpotential of the $\mu\nu$ SSM is given as [94, 95]

$$W = \epsilon_{ab} \left(Y_{u_{ij}} \hat{H}_u^b \hat{Q}_i^a \hat{u}_j^c + Y_{d_{ij}} \hat{H}_d^a \hat{Q}_i^b \hat{d}_j^c + Y_{e_{ij}} \hat{H}_d^a \hat{L}_i^b \hat{e}_j^c \right) \\ + \epsilon_{ab} Y_{\nu_{ij}} \hat{H}_u^b \hat{L}_i^a \hat{\nu}_j^c - \epsilon_{ab} \lambda_i \hat{\nu}_i^c \hat{H}_d^a \hat{H}_u^b + \frac{1}{3} \kappa_{ijk} \hat{\nu}_i^c \hat{\nu}_j^c \hat{\nu}_k^c. \quad (2)$$

where $a, b = 1, 2$ are SU(2) indices with antisymmetric tensor $\epsilon_{12} = 1$, and $i, j, k = 1, 2, 3$ are generation indices. The repeating indices imply the summation convention in the following.

$Y_{u,d,e,\nu}$, λ , and κ are dimensionless matrices, a vector, and a symmetric tensor. In the superpotential, the effective bilinear terms $\epsilon_{ab}\varepsilon_i\hat{H}_u^b\hat{L}_i^a$ and $\epsilon_{ab}\mu\hat{H}_d^a\hat{H}_u^b$ can be generated, with $\varepsilon_i = Y_{\nu_{ij}} \langle \tilde{\nu}_j^c \rangle$ and $\mu = \lambda_i \langle \tilde{\nu}_i^c \rangle$, once the electroweak symmetry is broken. In the $\mu\nu$ SSM, the general soft SUSY-breaking terms, the usual D - and F -term contributions of the tree-level scalar potential, and the mass matrices of the particles can be seen in Refs. [95, 96, 99]. In the $\mu\nu$ SSM, the gravitino or the axino can be the dark matter candidates [95, 96, 110, 114–119].

In our previous work, the Higgs boson mass and decay modes $h \rightarrow \gamma\gamma$, $h \rightarrow VV^*$ ($V = Z, W$), $h \rightarrow f\bar{f}$ ($f = b, \tau$), and $h \rightarrow Z\gamma$ in the $\mu\nu$ SSM have been researched [120–124]. Constrained by the 125 GeV Higgs boson mass and decays, here we will investigate the anomalous MDM of the charged leptons at two-loop level in the $\mu\nu$ SSM, combined with the updated experimental average of the muon MDM. For the electron anomalous MDM, $a_e = (g_e - 2)/2$, the experimental result showed a negative $\sim 2.4\sigma$ discrepancy between the measured value [125] and the SM prediction [126]. However, a new determination of the fine structure constant with a higher accuracy [127], obtained from the measurement of the recoil velocity on rubidium atoms, resulted into a re-evaluation of a_e in the SM, bringing to a positive $\sim 1.6\sigma$ discrepancy

$$\Delta a_e \equiv a_e^{exp} - a_e^{SM} = (4.8 \pm 3.0) \times 10^{-13}. \quad (3)$$

Interestingly, Now Δa_e and Δa_μ are all positive.

Now, the measured averages of the signal strengths for the 125 GeV Higgs boson decays into two taus and bottom quarks relative to the standard model (SM) prediction are respectively $1.15^{+0.16}_{-0.15}$ and 1.04 ± 0.13 with high experimental precision [128]. Although the Higgs boson decays to a pair of fermions of the third generation are now measured accurately by the Large Hadron Collider (LHC), the Higgs boson decays to a pair of fermions of the first or second generation are challenging to measure, due that the Yukawa couplings of the 125 GeV Higgs boson to fermions of the first and second generation are small than that of the third generation. However, the ATLAS and CMS Collaborations recently measured the 125 GeV Higgs boson decay to a pair of muons $h \rightarrow \mu\bar{\mu}$, which reported the signal strength relative to the SM prediction is 1.2 ± 0.6 with 2.0σ [129] and $1.19^{+0.40+0.15}_{-0.39-0.14}$ with 3.0σ [130], respectively. The dimuon decay of the 125 GeV Higgs boson $h \rightarrow \mu\bar{\mu}$ offers the best oppor-

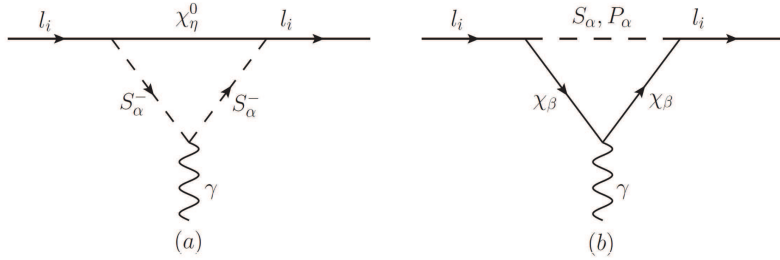


FIG. 1: The dominant one-loop diagrams, represent the contributions from neutral fermions χ_η^0 and charged scalars S_α^- loops (a), and the contributions from charged fermions χ_β and neutral scalars S_α (or P_α) loops (b).

tunity to measure the Higgs interactions with the second-generation fermions at the LHC. Within various theoretical frameworks, the 125 GeV Higgs boson decay $h \rightarrow \mu\bar{\mu}$ has been discussed [131–143]. Here, we will investigate the 125 GeV Higgs boson decay $h \rightarrow \mu\bar{\mu}$ at one-loop level in the $\mu\nu$ SSM.

In the following, we briefly introduce the MDM of the charged leptons in Sec. II. In Sec. III, we give the decay width of the 125 GeV Higgs boson decays to a pair of charged leptons $h \rightarrow l_i\bar{l}_i$ at one-loop level. Sec. IV and Sec. V respectively show the numerical analysis and summary.

II. THE MDM OF THE CHARGED LEPTONS

The MDM of the charged leptons in the $\mu\nu$ SSM can be written by the effective Lagrangian

$$\mathcal{L}_{MDM} = \frac{e}{4m_{l_i}} a_{l_i} \bar{l}_i \sigma^{\alpha\beta} l_i F_{\alpha\beta}, \quad (4)$$

where l_i represents the charged leptons which is on-shell, m_{l_i} is the mass of the charged leptons, $\sigma^{\alpha\beta} = \frac{i}{2}[\gamma^\alpha, \gamma^\beta]$, $F_{\alpha\beta}$ denotes the electromagnetic field strength and the MDM of the charged leptons is $a_{l_i} = \frac{1}{2}(g_{l_i} - 2)$. Including main two-loop electroweak corrections, the MDM of the charged leptons in the $\mu\nu$ SSM can be given by

$$a_{l_i}^{\text{SUSY}} = a_{l_i}^{\text{one-loop}} + a_{l_i}^{\text{two-loop}}, \quad (5)$$

where the one-loop corrections $a_{l_i}^{\text{one-loop}}$ are pictured in Fig. 1 and the main two-loop corrections $a_{l_i}^{\text{two-loop}}$ are showed in Fig. 2.

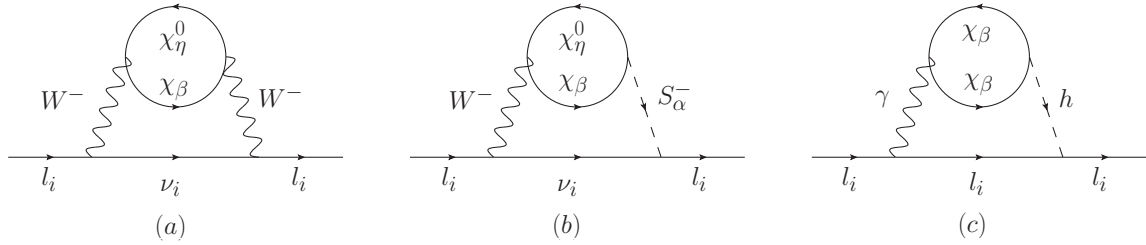


FIG. 2: The main two-loop rainbow diagram (a) and Barr-Zee type diagrams (b,c).

In Fig. 1, the contributions to the MDM of the charged leptons at the one-loop level in the $\mu\nu$ SUSY come from the neutral fermions and charged scalars loops (neutral fermions χ_η^0 and charged scalars S_α^- are loop particles) and the charged fermions and neutral scalars loop (charged fermions χ_β and neutral scalars $N_\alpha = S_\alpha, P_\alpha$ are loop particles). The concrete expressions of the one-loop corrections $a_{l_i}^{\text{one-loop}}$ can be found in our previous related work [122], where one can use the charged leptons l_i replace the muon l_μ .

Here, the dominant contribution of the muon MDM a_μ comes from the charged fermions and neutral scalars loops in Fig. 1(b). We check that the one-loop correction in the $\mu\nu$ SUSY is approximately in agreement with the MSSM and the Next-to-Minimal Supersymmetric Standard Model (NMSSM) [10, 64, 82]. Although the MDM of the muon in the $\mu\nu$ SUSY has roughly the same properties in the MSSM and NMSSM, it is subject to significantly relaxed limitations for the parameter space in the $\mu\nu$ SUSY if researching the other physical quantities. Of course, through introducing three singlet right-handed neutrino superfields $\hat{\nu}_i^c$ ($i = 1, 2, 3$) to solve the μ problem of the MSSM and generate three tiny neutrino masses, the $\mu\nu$ SUSY still can give some additional contributions to the muon MDM a_μ beyond the MSSM.

In Fig. 2, the main two-loop rainbow diagram (a) and Barr-Zee type diagrams (b,c) of a_{l_i} in the $\mu\nu$ SUSY are showed, which a closed fermion loop is attached to the virtual gauge bosons or scalars, and the corresponding corrections to a_{l_i} are obtained by attaching a photon on all possible ways to the internal particles. In our previous work [123], we show the main two-loop contributions of the muon MDM in the approximation $m_{\chi_\eta^0} \simeq m_{\chi_\beta}$. In this paper, we give the main two-loop contributions $a_{l_i}^{\text{two-loop}}$ in the general case.

In the $\mu\nu$ SUSY, the main SUSY two-loop corrections of the MDM of the charged leptons

can be given as

$$a_{l_i}^{\text{two-loop}} = a_{l_i}^{WW} + a_{l_i}^{WS} + a_{l_i}^{\gamma^h}, \quad (6)$$

where the terms $a_{l_i}^{WW}$, $a_{l_i}^{WS}$, $a_{l_i}^{\gamma^h}$ are the contributions corresponding to Fig. 2 (a-c). The contribution from the main two-loop rainbow diagram in Fig. 2 (a) can be written by

$$\begin{aligned} a_{l_i}^{WW} = & \frac{G_F m_{l_i}^2}{8\sqrt{2}\pi^4} \left\{ \left(|C_L^{W\bar{\chi}_\eta^0\chi_\beta}|^2 + |C_R^{W\bar{\chi}_\eta^0\chi_\beta}|^2 \right) T_1(1, x_{\chi_\eta^0}, x_{\chi_\beta}) \right. \\ & + \left(|C_L^{W\bar{\chi}_\eta^0\chi_\beta}|^2 - |C_R^{W\bar{\chi}_\eta^0\chi_\beta}|^2 \right) T_2(1, x_{\chi_\eta^0}, x_{\chi_\beta}) \\ & \left. + 2(x_{\chi_\eta^0} x_{\chi_\beta})^{1/2} \Re(C_R^{W\bar{\chi}_\eta^0\chi_\beta *} C_L^{W\bar{\chi}_\eta^0\chi_\beta}) T_3(1, x_{\chi_\eta^0}, x_{\chi_\beta}) \right\}, \end{aligned} \quad (7)$$

with $x_i = m_i^2/m_W^2$. The expressions of form factors T_i can be found in Refs. [144–146]. Here, the concrete expressions for couplings C in the $\mu\nu$ SSM can be seen in Ref. [99].

The contribution from the main two-loop Barr-Zee type diagram in Fig. 2 (b) can be given by

$$\begin{aligned} a_{l_i}^{WS} = & \frac{G_F m_{l_i} m_W}{128\pi^4 g_2} \Re(C_L^{S_\alpha^- \bar{l}_i \chi_{2+i}^0}) \\ & \times \left\{ (x_{\chi_\beta})^{1/2} F_1(1, x_{S_\alpha^-}, x_{\chi_\eta^0}, x_{\chi_\beta}) \Re(C_L^{S_\alpha^- \bar{\chi}_\beta \chi_\eta^0} C_L^{W\bar{\chi}_\eta^0\chi_\beta} + C_R^{S_\alpha^- \bar{\chi}_\beta \chi_\eta^0} C_R^{W\bar{\chi}_\eta^0\chi_\beta}) \right. \\ & + (x_{\chi_\eta^0})^{1/2} F_2(1, x_{S_\alpha^-}, x_{\chi_\eta^0}, x_{\chi_\beta}) \Re(C_L^{S_\alpha^- \bar{\chi}_\beta \chi_\eta^0} C_R^{W\bar{\chi}_\eta^0\chi_\beta} + C_R^{S_\alpha^- \bar{\chi}_\beta \chi_\eta^0} C_L^{W\bar{\chi}_\eta^0\chi_\beta}) \\ & + (x_{\chi_\beta})^{1/2} F_3(1, x_{S_\alpha^-}, x_{\chi_\eta^0}, x_{\chi_\beta}) \Re(C_L^{S_\alpha^- \bar{\chi}_\beta \chi_\eta^0} C_L^{W\bar{\chi}_\eta^0\chi_\beta} - C_R^{S_\alpha^- \bar{\chi}_\beta \chi_\eta^0} C_R^{W\bar{\chi}_\eta^0\chi_\beta}) \\ & \left. + (x_{\chi_\eta^0})^{1/2} F_4(1, x_{S_\alpha^-}, x_{\chi_\eta^0}, x_{\chi_\beta}) \Re(C_L^{S_\alpha^- \bar{\chi}_\beta \chi_\eta^0} C_R^{W\bar{\chi}_\eta^0\chi_\beta} - C_R^{S_\alpha^- \bar{\chi}_\beta \chi_\eta^0} C_L^{W\bar{\chi}_\eta^0\chi_\beta}) \right\}, \end{aligned} \quad (8)$$

where the expressions of form factors F_i can be seen in Ref. [144]. Here, in the $\mu\nu$ SSM, h denotes S_1 , l_i is denoted to χ_{2+i} . Considered that the masses of the charged scalars S_α^- are more larger than the mass of W gauge boson constrained by the present experiments, the contribution from the main two-loop Barr-Zee type diagram $a_{l_i}^{WS}$ is more smaller than the contribution from the main two-loop rainbow diagram $a_{l_i}^{WW}$.

The contribution from the main two-loop Barr-Zee type diagram in Fig. 2 (c) can be written as

$$a_{l_i}^{\gamma^h} = \frac{-G_F m_{l_i} m_W s_W^2}{16\pi^4} (x_{\chi_\beta})^{1/2} T_{11}(x_h, x_{\chi_\beta}, x_{\chi_\beta}) \Re(C_L^{h\bar{l}_i l_i} C_L^{h\bar{\chi}_\beta \chi_\beta}). \quad (9)$$

Through the numerical calculation, normalized to the one-loop corrections $a_{l_i}^{\text{one-loop}}$, the two-loop corrections of the MDM $a_{l_i}^{\text{two-loop}}$ in the $\mu\nu\text{SSM}$ may reach about 10%, when $\tan \beta$ is large and the masses of superpartners are small constrained from the experiments. So, one-loop correction alone is sufficient to explain the g-2 of the muon and satisfy other experimental constraints. In the following numerical analysis, the two-loop corrections of the muon MDM are still considered to be more precise.

III. $h \rightarrow l_i \bar{l}_i$ IN THE $\mu\nu\text{SSM}$

The corresponding effective amplitude for 125 GeV Higgs decay $h \rightarrow l_i \bar{l}_i$ can be written as

$$\mathcal{M} = h \bar{l}_i (F_L^i P_L + F_R^i P_R) l_i. \quad (10)$$

The decay width of $h \rightarrow l_i \bar{l}_i$ can be obtained as

$$\Gamma(h \rightarrow l_i \bar{l}_i) \simeq \frac{m_h}{16\pi} \left(|F_L^i|^2 + |F_R^i|^2 \right). \quad (11)$$

The contribution from the tree level in the $\mu\nu\text{SSM}$ can be written as

$$F_L^{(tree)i} = F_R^{(tree)i} = \frac{m_{l_i}}{\sqrt{2}v \cos \beta} R_{S_{11}}, \quad (12)$$

where m_{l_i} denotes the mass of the lepton l_i , $v \simeq 174\text{GeV}$, R_S is the unitary matrix which diagonalizes the mass matrix of CP-even neutral scalars [120]. For the SM, the contribution from the tree level can be written by

$$F_{L(\text{SM})}^{(tree)i} = F_{R(\text{SM})}^{(tree)i} = \frac{m_{l_i}}{\sqrt{2}v}. \quad (13)$$

The running lepton masses $m_{l_i}(\Lambda)$ are related to the pole masses m_{l_i} through [147]

$$m_{l_i}(\Lambda) = m_{l_i} \left\{ 1 - \frac{\alpha(\Lambda)}{\pi} \left[1 + \frac{3}{4} \ln \frac{\Lambda^2}{m_{l_i}^2} \right] \right\}. \quad (14)$$

Similarly to the decays $h \rightarrow l_i \bar{l}_i$, the decay width of the 125 GeV Higgs decay to the down-type quarks $h \rightarrow d_i \bar{d}_i$ can be given as

$$\Gamma(h \rightarrow d_i \bar{d}_i) \simeq \frac{N_c m_h}{16\pi} \left(|F_{dL}^i|^2 + |F_{dR}^i|^2 \right), \quad (15)$$

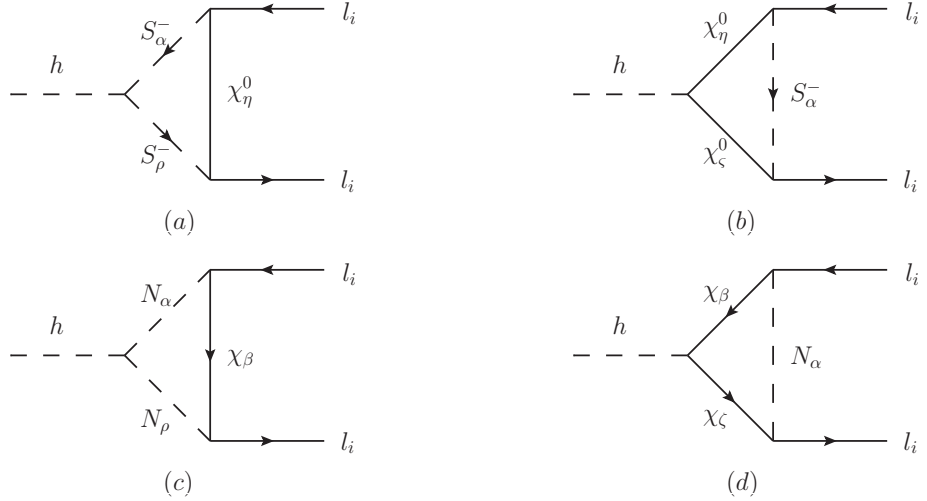


FIG. 3: The one-loop diagrams for $h \rightarrow l_i \bar{l}_i$ in the $\mu\nu$ SSM. (a,b) represent the contributions from charged scalar $S_{\alpha,\rho}^-$ and neutral fermion $\chi_{\eta,\varsigma}^0$ loops, while (c,d) represent the contributions from neutral scalar $N_{\alpha,\rho}$ ($N = S, P$) and charged fermion $\chi_{\beta,\varsigma}$ loops.

with $N_c = 3$, and the tree level contribution in the $\mu\nu$ SSM is

$$F_{dL}^{(tree)i} = F_{dR}^{(tree)i} = \frac{m_{d_i}}{\sqrt{2}v \cos \beta} R_{S_{11}}, \quad (16)$$

where m_{d_i} denotes the mass of the down-type quarks d_i . For the SM, the contribution from the tree level can be written by

$$F_{dL(\text{SM})}^{(tree)i} = F_{dR(\text{SM})}^{(tree)i} = \frac{m_{d_i}}{\sqrt{2}v}. \quad (17)$$

The difference of the decay width of $h \rightarrow f_i \bar{f}_i$ of the $\mu\nu$ SSM ($\Gamma_{\text{NP}}(h \rightarrow f_i \bar{f}_i)$) and that of the SM ($\Gamma_{\text{SM}}(h \rightarrow f_i \bar{f}_i)$) in the tree level can be given as

$$\delta_{tree} \equiv \frac{\Gamma_{\text{NP}}(h \rightarrow f_i \bar{f}_i) - \Gamma_{\text{SM}}(h \rightarrow f_i \bar{f}_i)}{\Gamma_{\text{SM}}(h \rightarrow f_i \bar{f}_i)} = \frac{R_{S_{11}}^2}{\cos^2 \beta} - 1. \quad (18)$$

Here $f_i = l_i$, d_i , due that the tree-level contribution of the Higgs boson decay into leptons is identical for the Higgs boson decay into down-type quarks. The numerical results can show that the ratio δ_{tree} can be about 1%, when the parameter $\tan \beta$ in the $\mu\nu$ SSM is small.

The one-loop electroweak correction for $h \rightarrow l_i \bar{l}_i$ in the SM is approximated by[133–137]

$$\Gamma_{SM}^{(one)}(h \rightarrow l_i \bar{l}_i) \simeq \Gamma_{SM}^{(tree)}(h \rightarrow l_i \bar{l}_i) \delta_{week}^l, \quad (19)$$

with

$$\delta_{week}^l = \frac{G_F}{8\pi^2\sqrt{2}} \left[7m_t^2 + m_W^2 \left(-5 + \frac{3\log c_W^2}{s_W^2} \right) - m_Z^2 \frac{6(1 - 8s_W^2 + 16s_W^4) - 1}{2} \right], \quad (20)$$

where the contributions come from t quark, W boson and Z boson. The numerical result shows that the one-loop electroweak contribution relative to the tree contribution δ_{week}^l is about 1.7%.

The one-loop diagrams for $h \rightarrow l_i \bar{l}_i$ in the $\mu\nu$ SSM beyond the SM are depicted by Fig. 3. Then, the contribution from the one-loop diagrams in the $\mu\nu$ SSM can be written by

$$F_{L,R}^{(one)i} = F_{L,R}^{(a)i} + F_{L,R}^{(b)i} + F_{L,R}^{(c)i} + F_{L,R}^{(d)i}, \quad (21)$$

where $F_{L,R}^{(a,b)i}$ denotes the contributions from charged scalar $S_{\alpha,\rho}^-$ and neutral fermion $\chi_{\eta,\varsigma}^0$ (upper index 0 shows neutral loops, and $F_{L,R}^{(c,d)i}$ stands for the contributions from the neutral scalar $N_{\alpha,\rho}$ ($N = S, P$) and charged fermion $\chi_{\beta,\varsigma}$ loops, respectively.

After integrating the heavy freedoms out, we formulate the neutral fermion loop contributions $F_{L,R}^{(a,b)i}$ as follows:

$$\begin{aligned} F_L^{(a)i} &= \frac{m_{\chi_\eta^0} C_{1\alpha\rho}^{S^\pm}}{m_W^2} C_L^{S_\rho^- \bar{l}_i \chi_\eta^0} C_L^{S_\alpha^- * \bar{\chi}_\eta^0 l_i} G_1(x_{\chi_\eta^0}, x_{S_\alpha^-}, x_{S_\rho^-}), \\ F_L^{(b)i} &= \frac{m_{\chi_\varsigma^0} m_{\chi_\eta^0}}{m_W^2} C_L^{S_\alpha^- \bar{l}_i \chi_\varsigma^0} C_L^{h \bar{\chi}_\varsigma^0 \chi_\eta^0} C_L^{S_\alpha^- * \bar{\chi}_\eta^0 l_i} G_1(x_{S_\alpha^-}, x_{\chi_\varsigma^0}, x_{\chi_\eta^0}) \\ &\quad + C_L^{S_\alpha^- \bar{l}_i \chi_\varsigma^0} C_R^{h \bar{\chi}_\varsigma^0 \chi_\eta^0} C_L^{S_\alpha^- * \bar{\chi}_\eta^0 l_i} G_2(x_{S_\alpha^-}, x_{\chi_\varsigma^0}, x_{\chi_\eta^0}), \\ F_R^{(a,b)i} &= F_L^{(a,b)i} \Big|_{L \leftrightarrow R}. \end{aligned} \quad (22)$$

Here, the concrete expressions for the couplings C can be found in Refs. [121, 122], and the loop functions G_i are given as

$$\begin{aligned} G_1(x_1, x_2, x_3) &= \frac{1}{16\pi^2} \left[\frac{x_1 \ln x_1}{(x_1 - x_2)(x_1 - x_3)} + \frac{x_2 \ln x_2}{(x_2 - x_1)(x_2 - x_3)} \right. \\ &\quad \left. + \frac{x_3 \ln x_3}{(x_3 - x_1)(x_3 - x_2)} \right], \end{aligned} \quad (23)$$

$$\begin{aligned} G_2(x_1, x_2, x_3) &= \frac{1}{16\pi^2} \left[\frac{x_1^2 \ln x_1}{(x_1 - x_2)(x_1 - x_3)} + \frac{x_2^2 \ln x_2}{(x_2 - x_1)(x_2 - x_3)} \right. \\ &\quad \left. + \frac{x_3^2 \ln x_3}{(x_3 - x_1)(x_3 - x_2)} \right]. \end{aligned} \quad (24)$$

In a similar way, the charged fermion loop contributions $F_{L,R}^{(c,d)i}$ are

$$\begin{aligned} F_L^{(c)i} &= \sum_{N=S,P} \frac{m_{\chi_\beta} C_{1\alpha\rho}^N}{m_W^2} C_L^{N_\rho \bar{l}_i \chi_\beta} C_L^{N_\alpha \bar{\chi}_\beta l_i} G_1(x_{\chi_\beta}, x_{N_\alpha}, x_{N_\rho}), \\ F_L^{(d)i} &= \sum_{N=S,P} \left[C_L^{N_\alpha \bar{l}_i \chi_\zeta} C_R^{h \bar{\chi}_\zeta \chi_\beta} C_L^{N_\alpha \bar{\chi}_\beta l_i} G_2(x_{N_\alpha}, x_{\chi_\zeta}, x_{\chi_\beta}) \right. \\ &\quad \left. + \frac{m_{\chi_\zeta} m_{\chi_\beta}}{m_W^2} C_L^{N_\alpha \bar{l}_i \chi_\zeta} C_L^{h \bar{\chi}_\zeta \chi_\beta} C_L^{N_\alpha \bar{\chi}_\beta l_i} G_1(x_{N_\alpha}, x_{\chi_\zeta}, x_{\chi_\beta}) \right], \\ F_R^{(c,d)i} &= F_L^{(c,d)i} \Big|_{L \leftrightarrow R}. \end{aligned} \quad (25)$$

IV. NUMERICAL ANALYSIS

Firstly, we take some appropriate parameter space in the $\mu\nu$ SSM. For soft SUSY-breaking mass squared parameters, we make the minimal flavor violation (MFV) assumptions

$$\begin{aligned} m_{\tilde{Q}_{ij}}^2 &= m_{\tilde{Q}_i}^2 \delta_{ij}, & m_{\tilde{u}_{ij}^c}^2 &= m_{\tilde{u}_i^c}^2 \delta_{ij}, & m_{\tilde{d}_{ij}^c}^2 &= m_{\tilde{d}_i^c}^2 \delta_{ij}, \\ m_{\tilde{L}_{ij}}^2 &= m_{\tilde{L}_i}^2 \delta_{ij}, & m_{\tilde{e}_{ij}^c}^2 &= m_{\tilde{e}_i^c}^2 \delta_{ij}, & m_{\tilde{\nu}_{ij}^c}^2 &= m_{\tilde{\nu}_i^c}^2 \delta_{ij}, \end{aligned} \quad (26)$$

where $i, j, k = 1, 2, 3$. $m_{\tilde{\nu}_i^c}^2$ can be constrained by the minimization conditions of the neutral scalar potential seen in Ref. [120]. For some coupling parameters, we also choose the MFV assumptions

$$\begin{aligned} \kappa_{ijk} &= \kappa \delta_{ij} \delta_{jk}, & (A_\kappa \kappa)_{ijk} &= A_\kappa \kappa \delta_{ij} \delta_{jk}, & v_{\nu_i^c} &= v_{\nu^c}, & \lambda_i &= \lambda, & (A_\lambda \lambda)_i &= A_\lambda \lambda, \\ Y_{e_{ij}} &= Y_{e_i} \delta_{ij}, & (A_e Y_e)_{ij} &= A_e Y_{e_i} \delta_{ij}, & Y_{\nu_{ij}} &= Y_{\nu_i} \delta_{ij}, & (A_\nu Y_\nu)_{ij} &= a_{\nu_i} \delta_{ij}, \end{aligned} \quad (27)$$

Through our previous work [113], we have discussed in detail how the neutrino oscillation data constrain left-handed sneutrino VEVs $v_{\nu_i} \sim \mathcal{O}(10^{-4} \text{ GeV})$ and neutrino Yukawa couplings $Y_{\nu_i} \sim \mathcal{O}(10^{-7})$ in the $\mu\nu$ SSM via the TeV scale seesaw mechanism. In the following, we choose $m_{\nu_1} = 10^{-2} \text{ eV}$ as the lightest neutrino and assume the neutrino mass spectrum with normal ordering, using neutrino oscillation experimental data [128] to constrain the parameters v_{ν_i} and Y_{ν_i} . Considered experimental data on quark mixing, one can have

$$\begin{aligned} Y_{u_{ij}} &= Y_{u_i} V_{L_{ij}}^u, & (A_u Y_u)_{ij} &= A_{u_i} Y_{u_{ij}}, \\ Y_{d_{ij}} &= Y_{d_i} V_{L_{ij}}^d, & (A_d Y_d)_{ij} &= A_d Y_{d_{ij}}, \end{aligned} \quad (28)$$

Parameters	Min	Max
$\tan \beta$	4	40
v_{ν^c}/TeV	1	6
M_2/TeV	0.3	2
$m_{\tilde{L}} = m_{\tilde{e}^c}/\text{TeV}$	0.5	2
$m_{\tilde{u}_3^c}/\text{TeV}$	1	4
A_t/TeV	1	4

TABLE I: Random scan parameters.

and $V = V_L^u V_L^{d\dagger}$ denotes the CKM matrix.

$$Y_{u_i} = \frac{m_{u_i}}{v_u}, \quad Y_{d_i} = \frac{m_{d_i}}{v_d}, \quad Y_{e_i} = \frac{m_{l_i}}{v_d}, \quad (29)$$

where the m_{u_i} , m_{d_i} and m_{l_i} stand for up-quark, down-quark and charged lepton masses.

Through analysis of the parameter space of the $\mu\nu$ SUSY [95], we can choose reasonable parameter values to be $\kappa = 0.4$, $A_\kappa = -300$ GeV, $\lambda = 0.1$, $A_\lambda = 500$ GeV and $A_{u_{1,2}} = A_d = A_e = 1$ TeV for simplicity. Considering the direct search for supersymmetric particles [128], we take $m_{\tilde{Q}_{1,2,3}} = m_{\tilde{u}_{1,2}^c} = m_{\tilde{d}_{1,2,3}^c} = 2$ TeV, $M_3 = 2.5$ TeV. For simplicity, we will choose the gauginos' Majorana masses $M_1 = M_2$. As key parameters, $A_{u_3} \equiv A_t$, $m_{\tilde{u}_3^c}$ and $\tan \beta \equiv v_u/v_d$ greatly affect the lightest Higgs boson mass. Therefore, the free parameters that affect our next analysis are

$$\tan \beta, \quad v_{\nu^c}, \quad M_2, \quad m_{\tilde{L}}, \quad m_{\tilde{e}^c}, \quad m_{\tilde{u}_3^c}, \quad A_t. \quad (30)$$

To present numerical analysis, we random scan the parameter space shown in Tab. I. Considered that the light stop mass is easily ruled out by the experiment, we scan the parameter $m_{\tilde{u}_3^c}$ from 1 TeV. Now the average measured mass of the Higgs boson is [128]

$$m_h = 125.25 \pm 0.17 \text{ GeV}, \quad (31)$$

where the accurate Higgs boson mass can give stringent constraint on parameter space for the model. In our previous work [120], the Higgs boson masses in the $\mu\nu$ SUSY including the main two-loop radiative corrections are discussed. Through the work, here the scanning results

are constrained by the lightest Higgs boson mass with $124.68 \text{ GeV} \leq m_h \leq 125.52 \text{ GeV}$, where a 3σ experimental error is considered. For the signal strengths of the light Higgs boson decay modes $h \rightarrow \gamma\gamma$, WW^* , ZZ^* , $b\bar{b}$, $\tau\bar{\tau}$, $\mu\bar{\mu}$, we adopt the averages of the results from PDG which reads [128]

$$\begin{aligned}\mu_{\gamma\gamma}^{exp} &= 1.11_{-0.09}^{+0.10}, & \mu_{WW^*}^{exp} &= 1.19 \pm 0.12, & \mu_{ZZ^*}^{exp} &= 1.06 \pm 0.09, \\ \mu_{b\bar{b}}^{exp} &= 1.04 \pm 0.13, & \mu_{\tau\bar{\tau}}^{exp} &= 1.15_{-0.15}^{+0.16}, & \mu_{\mu\bar{\mu}}^{exp} &= 1.19 \pm 0.34.\end{aligned}\quad (32)$$

Here a 2σ experimental error will be considered in the scanning results, using our previous work [121] on the signal strengths of the Higgs boson decay channels $h \rightarrow \gamma\gamma$, $h \rightarrow VV^*$ ($V = Z, W$), and $h \rightarrow f\bar{f}$ ($f = b, \tau$) in the $\mu\nu\text{SSM}$.

There is a close similarity between the anomalous MDM of muon and the branching ratio of $\bar{B} \rightarrow X_s\gamma$ in the supersymmetric model [14]. They both get large $\tan\beta$ enhancements from the down-fermion Yukawa couplings, $Y_{d_i} = m_{d_i}/v_d = m_{d_i}\sqrt{\tan^2\beta + 1}/v$ and $Y_{e_i} = m_{l_i}/v_d = m_{l_i}\sqrt{\tan^2\beta + 1}/v$ with $v = \sqrt{v_d^2 + v_u^2} \simeq 174 \text{ GeV}$. Combined with the experimental data from CLEO [148], BELLE [149, 150] and BABAR [151–153], the current experimental value for the branching ratio of $\bar{B} \rightarrow X_s\gamma$ is [128]

$$\text{Br}(\bar{B} \rightarrow X_s\gamma) = (3.49 \pm 0.19) \times 10^{-4}. \quad (33)$$

Using our previous work about the rare decay $\bar{B} \rightarrow X_s\gamma$ in the $\mu\nu\text{SSM}$ [154], the following results in the scanning are also constrained by $2.92 \times 10^{-4} \leq \text{Br}(\bar{B} \rightarrow X_s\gamma) \leq 4.06 \times 10^{-4}$, where a 3σ experimental error is considered.

A. The MDM of charged leptons

Firstly, to illustrate clearly the cross-correlation of the model parameters, we plot a_μ^{SUSY} varying with v_{ν^c} with different M_2 and $\tan\beta$ in Fig. 4, choosing $m_{\tilde{L}} = m_{\tilde{e}^c} = 0.7 \text{ TeV}$ and $m_{\tilde{u}_3^c} = A_t = 1 \text{ TeV}$ for simplicity. In Fig 4(a), the solid line denotes $M_2 = 0.3 \text{ TeV}$, the dashed line denotes $M_2 = 1 \text{ TeV}$, and the dotted line denotes $M_2 = 2 \text{ TeV}$, with $\tan\beta = 40$. The numerical results show that the muon anomalous MDM a_μ^{SUSY} is decoupling with increasing v_{ν^c} or M_2 , which can affect the masses of the charginos and neutralinos. In

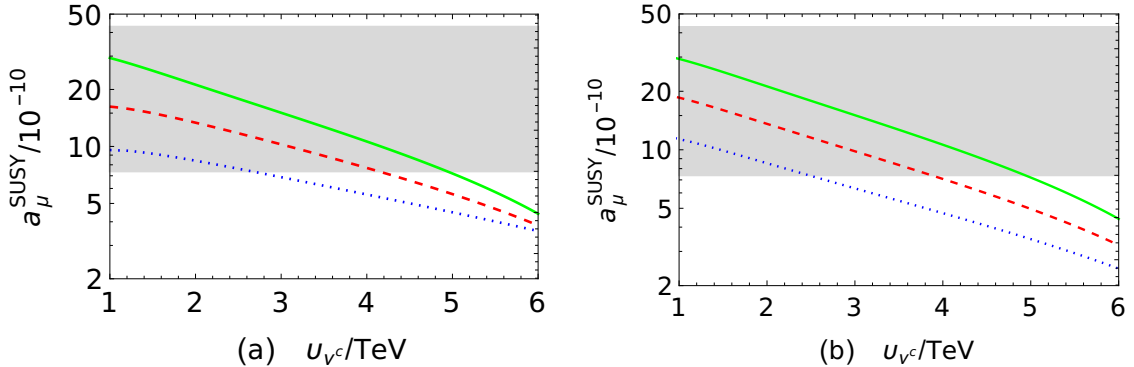


FIG. 4: (Color online) a_μ^{SUSY} versus v_{ν^c} with different M_2 (a) and $\tan\beta$ (b), where the gray area denotes Δa_μ at 3.0σ given in Eq. (1).

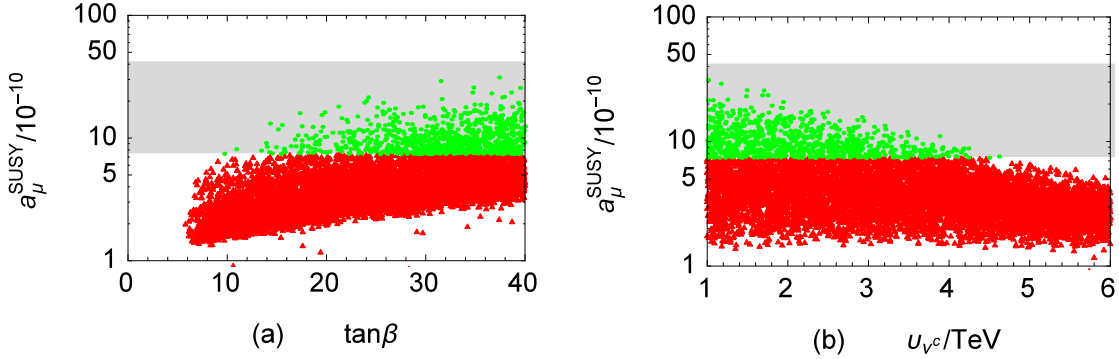


FIG. 5: (Color online) a_μ^{SUSY} versus $\tan\beta$ (a) and v_{ν^c} (b), where the gray area denotes Δa_μ at 3.0σ given in Eq. (1) and the red triangles are eliminated.

Fig 4(b), the solid line represents $\tan\beta = 40$, the dashed line represents $\tan\beta = 25$, and the dotted line represents $\tan\beta = 15$, with $M_2 = 0.3$ TeV. Through Fig 4(b), we can see that the muon anomalous MDM a_μ^{SUSY} get large $\tan\beta$ enhancements, which is similar with that of the MSSM.

Through random scanning the parameter space shown in Tab. I, we plot anomalous magnetic dipole moment of muon a_μ^{SUSY} varying with the key parameters $\tan\beta$ (a) and v_{ν^c} (b) in Fig. 5, where the gray area denotes Δa_μ at 3.0σ given in Eq. (1). Here, the red triangles are excluded by Δa_μ at 3.0σ . The green points of the $\mu\nu$ SSM are accord with Δa_μ at 3.0σ , which can explain the current tension between the experimental measurement and the SM theoretical prediction for the muon anomalous MDM.

Fig. 5(a) show that the muon anomalous MDM a_μ^{SUSY} increases with increasing of the

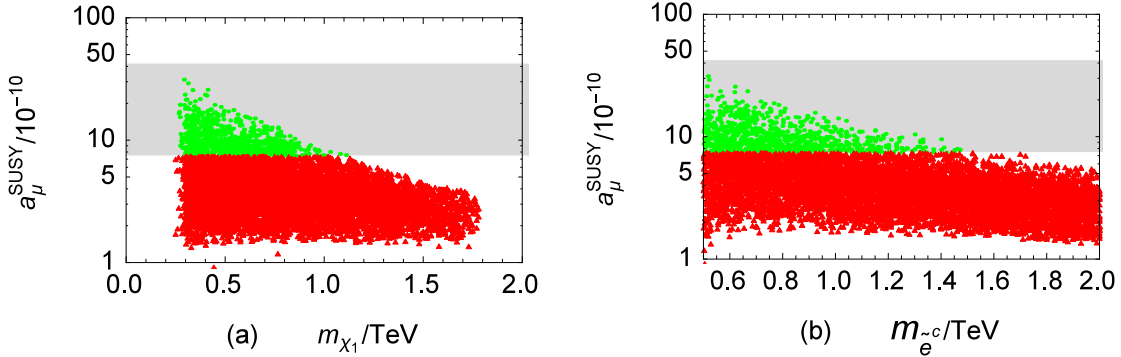


FIG. 6: (Color online) a_μ^{SUSY} versus m_{χ_1} (a) and $m_{\tilde{e}^c}$ (b), where the gray area denotes Δa_μ at 3.0σ given in Eq. (1) and the red triangles are eliminated.

parameter $\tan \beta$. One can find that a significant region of the parameter space is excluded by Δa_μ at 3.0σ in the small $\tan \beta$ region. Here, very small $\tan \beta$ region is also easily eliminated by the constraint of the 125 GeV Higgs boson mass. The numerical results in Fig. 5(b) depict that the muon anomalous MDM a_μ^{SUSY} is decoupling with increasing of v_{ν^c} . Due that v_{ν^c} can affect the masses of charginos and neutralinos. We can see that the value of the muon anomalous MDM a_μ^{SUSY} in the $\mu\nu$ SSM could explain the experimental muon anomalous MDM Δa_μ at 3.0σ shown in Eq. (1), when v_{ν^c} is small and $\tan \beta$ is large. Constrained by Δa_μ at 3.0σ shown in Eq. (1), $\tan \beta < 10$ or $v_{\nu^c} > 5$ TeV will easily be eliminated.

To see more clearly, we plot anomalous magnetic dipole moment of muon a_μ^{SUSY} varying with the lightest chargino mass m_{χ_1} in Fig. 6(a), through scanning the parameter space shown in Tab. I. The results show that the contribution of the lightest chargino mass m_{χ_1} is roughly similar with the contribution of the parameter v_{ν^c} . Because here $\mu \equiv 3\lambda v_{\nu^c}$, where μ directly affect the masses of the charginos. In Fig. 6(b), a_μ^{SUSY} versus $m_{\tilde{e}^c}$ is also pictured. When $m_{\tilde{e}^c}$ is small, a_μ^{SUSY} in the $\mu\nu$ SSM could explain the Δa_μ at 3.0σ . The variation trend of a_μ^{SUSY} versus $m_{\tilde{e}^c}$ coincides with the decoupling theorem, due that $m_{\tilde{e}^c}$ directly affects the masses of the slepton. One can see that anomalous magnetic dipole moment of muon a_μ^{SUSY} can reach Δa_μ at 3.0σ shown in Eq. (1), when $m_{\chi_1} < 1.1$ TeV and $m_{\tilde{e}^c} < 1.5$ TeV.

For the anomalous MDM of the electron and tau lepton, we also picture a_μ^{SUSY} versus a_e^{SUSY} (a) and a_τ^{SUSY} (b) in Fig. 7, where the green points are in agree with Δa_μ at 3.0σ given in Eq. (1) and the red triangles are eliminated by that. Constrained by the updated

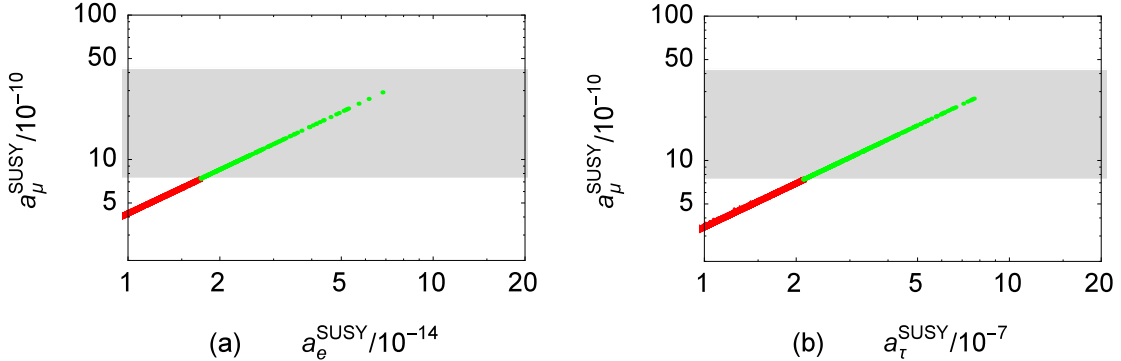


FIG. 7: (Color online) a_μ^{SUSY} versus a_e^{SUSY} (a) and a_τ^{SUSY} (b), where the gray area denotes Δa_μ at 3.0σ given in Eq. (1) and the red triangles are eliminated by Δa_μ at 3.0σ .

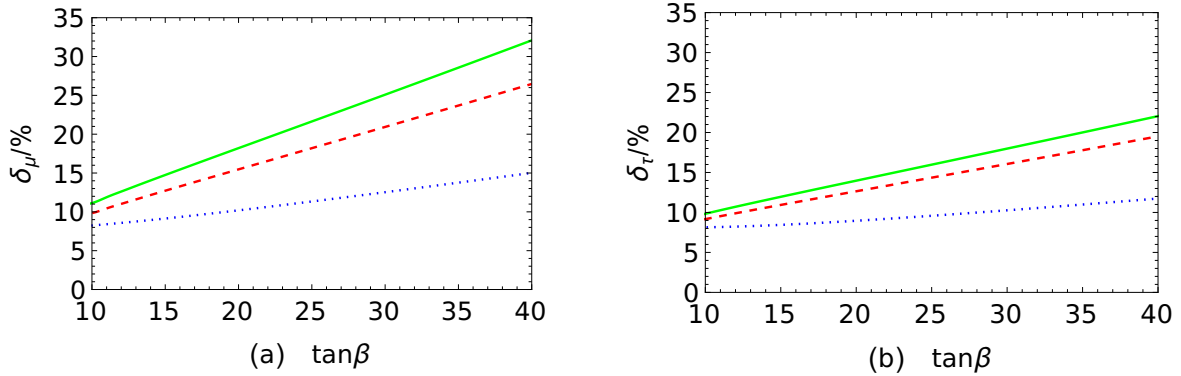


FIG. 8: (Color online) The ratio δ_μ (a) and δ_τ (b) versus the parameter $\tan \beta$ with different v_{ν^c} .

discrepancy for Δa_μ at 3.0σ , the anomalous MDM a_e^{SUSY} and a_τ^{SUSY} in the $\mu\nu\text{SSM}$ can be about 0.7×10^{-13} and 0.8×10^{-6} , respectively. The numerical results show that the ratio between the anomalous MDMs of the tau lepton and muon is about 2.8×10^2 , which is in agree with $\frac{\Delta a_\tau}{\Delta a_\mu} \simeq m_\tau^2/m_\mu^2 \simeq 2.8 \times 10^2$. The ratio between the anomalous MDMs of the muon and electron also is consistent with $\frac{\Delta a_\mu}{\Delta a_e} \simeq m_\mu^2/m_e^2 \simeq 4.3 \times 10^4$.

B. $h \rightarrow l_i \bar{l}_i$

We define the physical quantity

$$\delta_{l_i} \equiv \frac{\Gamma_{\text{NP}}(h \rightarrow l_i \bar{l}_i) - \Gamma_{\text{SM}}(h \rightarrow l_i \bar{l}_i)}{\Gamma_{\text{SM}}(h \rightarrow l_i \bar{l}_i)}, \quad (34)$$

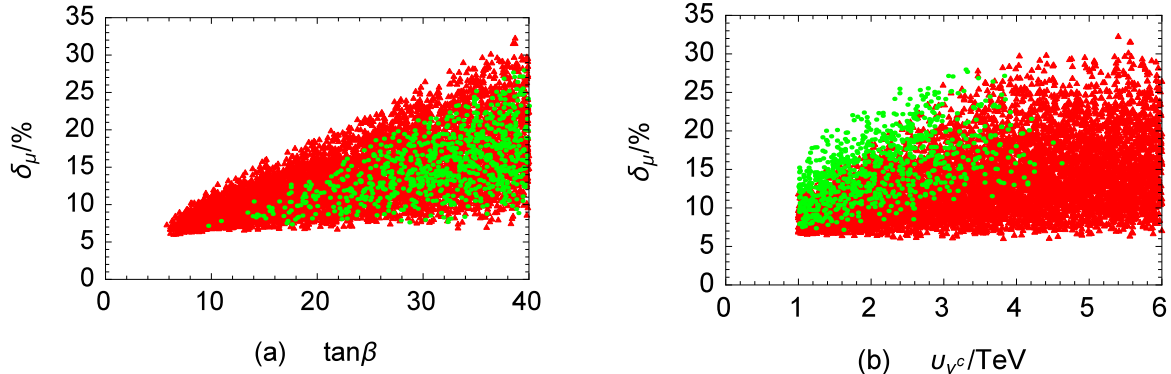


FIG. 9: (Color online) The ratio δ_μ versus the parameter $\tan\beta$ (a) and v_{ν^c} (b).

to show the difference of the decay width of $h \rightarrow l_i \bar{l}_i$ of the $\mu\nu$ SSM ($\Gamma_{\text{NP}}(h \rightarrow l_i \bar{l}_i)$) and that of the SM ($\Gamma_{\text{SM}}(h \rightarrow l_i \bar{l}_i)$), where $l_i = e, \mu, \tau$. Firstly, to illustrate clearly the cross-correlation of the model parameters, we plot the ratio δ_μ (a) and δ_τ (b) versus the parameter $\tan\beta$ with different v_{ν^c} in Fig. 8, taking $m_{\tilde{L}} = m_{\tilde{e}^c} = 0.6$ TeV, $M_2 = 2$ TeV, $m_{\tilde{u}_3^c} = 2$ TeV and $A_t = 3$ TeV for simplicity. In Fig. 8, the solid line denotes $v_{\nu^c} = 6$ TeV, the dashed line denotes $v_{\nu^c} = 3$ TeV, and the dotted line denotes $v_{\nu^c} = 1$ TeV, respectively. The numerical results in Fig. 8 show that the ratio δ_μ and δ_τ increase with increasing of $\tan\beta$ or v_{ν^c} . The charged leptons Yukawa couplings get large $\tan\beta$ enhancements, with $Y_{e_i} = m_{l_i} \sqrt{\tan^2 \beta + 1}/v$.

Through scanning in Tab. I, we plot Figs. 9-10, where the green dots are the corresponding physical quantity's values of the remaining parameters after being constrained by the muon anomalous MDM a_μ^{SUSY} in the $\mu\nu$ SSM with $7.4 \times 10^{-10} \leq a_\mu^{\text{SUSY}} \leq 42.8 \times 10^{-10}$ considered a 3σ experimental error. The red triangles are ruled out by the muon anomalous MDM with $a_\mu^{\text{SUSY}} > 42.8 \times 10^{-10}$ and $a_\mu^{\text{SUSY}} < 7.4 \times 10^{-10}$.

In Fig. 9, we plot the ratio δ_μ varying with the parameter $\tan\beta$ (a) and v_{ν^c} (b). We can see that the ratio δ_μ will increase with increasing of $\tan\beta$ in Fig. 9(a). The ratio δ_μ can be close to 30% when the parameter $\tan\beta$ is large, Constrained by Δa_μ at 3.0σ . In Fig. 9(b) shows that the ratio δ_μ is non-decoupling with increasing v_{ν^c} . The maximum of the ratio δ_μ can be around 15% as v_{ν^c} is about 1 TeV and close to 30% as v_{ν^c} is about 3 TeV. In the $\mu\nu$ SSM, the parameter v_{ν^c} leads to the mixing of the neutral components of the Higgs doublets with the sneutrinos. The mixing affects the lightest Higgs boson mass and the Higgs couplings, which is different from the SM.

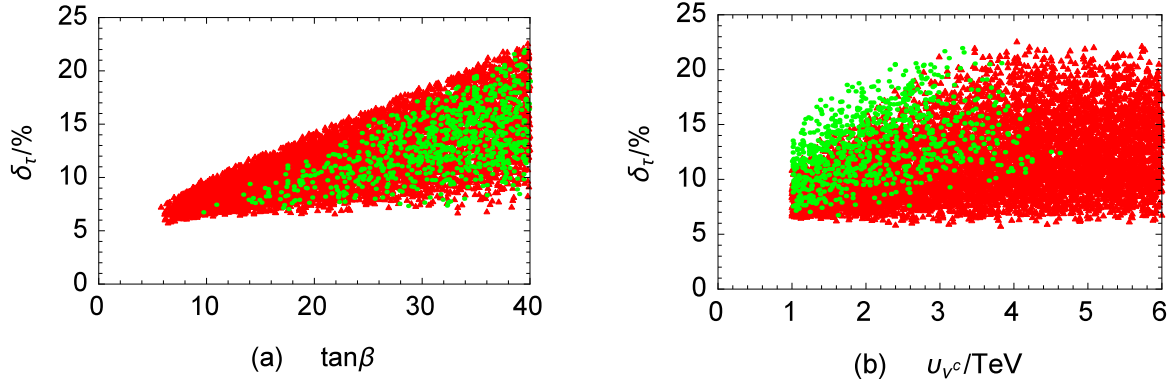


FIG. 10: (Color online) The ratio δ_τ versus the parameter $\tan\beta$ (a) and v_{ν^c} (b).

In addition, we plot the ratio δ_τ varying with the parameter $\tan\beta$ and v_{ν^c} in Fig. 10, which the variation trend is similar with that of the ratio δ_μ . The numerical results show that, constrained by the experimental value of the muon anomalous MDM, the ratio δ_τ can be about 20%, when $\tan\beta$ is about 40 and v_{ν^c} is around 3 TeV.

V. SUMMARY

Considered that the new experimental average for the muon anomalous MDM increases the tension between experiment and SM prediction to 4.2σ , we analyse the muon anomalous MDM at two-loop level in the $\mu\nu$ SSM. The numerical results show that the $\mu\nu$ SSM can explain the current tension between the experimental measurement and the SM theoretical prediction for the muon anomalous MDM, constrained by the 125 GeV Higgs boson mass and decays, the rare decay $\bar{B} \rightarrow X_s\gamma$ and so on. The new experimental average of the muon anomalous MDM considered a 3σ also give a strictly constraint for the parameter space of the $\mu\nu$ SSM, which constrain that $\tan\beta > 10$, $m_{\tilde{e}^c} < 1.5$ TeV and $v_{\nu^c} < 5$ TeV with $\lambda = 0.1$. And the anomalous MDM of tau lepton and electron in the $\mu\nu$ SSM can reach about 0.7×10^{-13} and 0.8×10^{-6} respectively, constrained by the new experimental average of the muon anomalous MDM at 3.0σ .

An upgrade to the Muon g-2 experiment at Fermilab and another experiment at J-PARC [155] will measure the muon anomalous magnetic dipole moment with higher precision, which may reach a 5σ deviation from the SM, constituting an augury for new physics beyond the

SM. And the anomalous MDM of tau lepton and electron whether deviate from the SM prediction will be given more accurately, with the development of experiment in the future.

Considered that the ATLAS and CMS Collaborations measured the 125 GeV Higgs boson decay to a pair of muons $h \rightarrow \mu\bar{\mu}$ recently, we also investigate the 125 GeV Higgs boson decay $h \rightarrow \mu\bar{\mu}$ at one-loop level in the $\mu\nu$ SSM. Compared to the SM prediction, the decay width of $h \rightarrow \mu\bar{\mu}$ and $h \rightarrow \tau\bar{\tau}$ in the $\mu\nu$ SSM can boost up about 30% and 20%, considering the constraint from the muon anomalous magnetic dipole moment. In the $\mu\nu$ SSM, the mixing of the neutral components of the Higgs doublets with the sneutrinos affects the lightest Higgs boson mass and the Higgs couplings, which can contribute to the Higgs boson decay. In the future, high luminosity or high energy large colliders [156–159] will detect the Higgs boson decay $h \rightarrow \mu\bar{\mu}$ and $h \rightarrow \tau\bar{\tau}$ with high precision, which may see the indication of new physics.

Acknowledgments

The work has been supported by the National Natural Science Foundation of China (NNSFC) with Grants No. 11705045, No. 11535002, No. 12075074, the youth top-notch talent support program of the Hebei Province, and Midwest Universities Comprehensive Strength Promotion project.

- [1] B. Abi et al. (Muon g-2 Collaboration), Phys. Rev. Lett. **126** (2021) 141801.
- [2] T. Albahri et al. (Muon g-2 Collaboration), Phys. Rev. D **103** (2021) 072002.
- [3] T. Albahri et al. (Muon g-2 Collaboration), Phys. Rev. A **103** (2021) 042208.
- [4] T. Albahri et al. (Muon g-2 Collaboration), Phys. Rev. Accel. Beams **24** (2021) 044002.
- [5] G.W. Bennett et al. (Muon g-2 Collaboration), Phys. Rev. D **73** (2006) 072003.
- [6] T. Aoyama *et al.*, Phys. Rept. **887**, 1-166 (2020) [arXiv:2006.04822 [hep-ph]].
- [7] F. Jegerlehner and A. Nyffeler, Phys. Rept. **477**, 1-110 (2009) [arXiv:0902.3360 [hep-ph]].
- [8] M. Davier, A. Hoecker, B. Malaescu and Z. Zhang, Eur. Phys. J. C **71**, 1515 (2011) [erratum: Eur. Phys. J. C **72**, 1874 (2012)] [arXiv:1010.4180 [hep-ph]].

- [9] S. Eidelman and F. Jegerlehner, Z. Phys. C **67**, 585-602 (1995) [arXiv:hep-ph/9502298 [hep-ph]].
- [10] T. Moroi, Phys. Rev. D **53**, 6565-6575 (1996) [erratum: Phys. Rev. D **56**, 4424 (1997)] [arXiv:hep-ph/9512396 [hep-ph]].
- [11] T. Aoyama, M. Hayakawa, T. Kinoshita and M. Nio, Phys. Rev. Lett. **109**, 111808 (2012) [arXiv:1205.5370 [hep-ph]].
- [12] K. Hagiwara, A. D. Martin, D. Nomura and T. Teubner, Phys. Lett. B **649**, 173-179 (2007) [arXiv:hep-ph/0611102 [hep-ph]].
- [13] J. Bijnens, E. Pallante and J. Prades, Nucl. Phys. B **474**, 379-420 (1996) [arXiv:hep-ph/9511388 [hep-ph]].
- [14] S. P. Martin and J. D. Wells, Phys. Rev. D **64**, 035003 (2001) [arXiv:hep-ph/0103067 [hep-ph]].
- [15] M. Lindner, M. Platscher and F. S. Queiroz, Phys. Rept. **731**, 1-82 (2018) [arXiv:1610.06587 [hep-ph]].
- [16] K. Hagiwara, A. D. Martin, D. Nomura and T. Teubner, Phys. Rev. D **69**, 093003 (2004) [arXiv:hep-ph/0312250 [hep-ph]].
- [17] J. Bijnens, E. Pallante and J. Prades, Nucl. Phys. B **626**, 410-411 (2002) [arXiv:hep-ph/0112255 [hep-ph]].
- [18] U. Chattopadhyay and P. Nath, Phys. Rev. D **53**, 1648-1657 (1996) [arXiv:hep-ph/9507386 [hep-ph]].
- [19] M. Davier, A. Hoecker, B. Malaescu and Z. Zhang, Eur. Phys. J. C **77** (2017) 827 [arXiv:1706.09436 [hep-ph]].
- [20] J. Bijnens, E. Pallante and J. Prades, Phys. Rev. Lett. **75** (1995), 1447-1450 [erratum: Phys. Rev. Lett. **75** (1995), 3781] [arXiv:hep-ph/9505251 [hep-ph]].
- [21] K. Hagiwara, A. D. Martin, D. Nomura and T. Teubner, Phys. Lett. B **557** (2003), 69-75 [arXiv:hep-ph/0209187 [hep-ph]].
- [22] M. Hayakawa, T. Kinoshita and A. I. Sanda, Phys. Rev. Lett. **75** (1995), 790-793 [arXiv:hep-ph/9503463 [hep-ph]].
- [23] L. L. Everett, G. L. Kane, S. Rigolin and L. T. Wang, Phys. Rev. Lett. **86** (2001), 3484-3487

[arXiv:hep-ph/0102145 [hep-ph]].

- [24] E. de Rafael, Phys. Lett. B **322** (1994), 239-246 [arXiv:hep-ph/9311316 [hep-ph]].
- [25] U. Chattopadhyay and P. Nath, Phys. Rev. Lett. **86** (2001), 5854-5857 [arXiv:hep-ph/0102157 [hep-ph]].
- [26] M. Hayakawa, T. Kinoshita and A. I. Sanda, Phys. Rev. D **54** (1996), 3137-3153 [arXiv:hep-ph/9601310 [hep-ph]].
- [27] J. Hisano and K. Tobe, Phys. Lett. B **510**, 197-204 (2001) [arXiv:hep-ph/0102315 [hep-ph]].
- [28] J. F. de Troconiz and F. J. Yndurain, Phys. Rev. D **65** (2002), 093001 [arXiv:hep-ph/0106025 [hep-ph]].
- [29] S. Baek, N. G. Deshpande, X. G. He and P. Ko, Phys. Rev. D **64** (2001), 055006 [arXiv:hep-ph/0104141 [hep-ph]].
- [30] H. Davoudiasl, H. S. Lee and W. J. Marciano, Phys. Rev. D **86** (2012), 095009 [arXiv:1208.2973 [hep-ph]].
- [31] M. J. Ramsey-Musolf and M. B. Wise, Phys. Rev. Lett. **89** (2002), 041601 [arXiv:hep-ph/0201297 [hep-ph]].
- [32] M. Benayoun, P. David, L. DelBuono and F. Jegerlehner, Eur. Phys. J. C **73** (2013), 2453 [arXiv:1210.7184 [hep-ph]].
- [33] G. Colangelo, M. Hoferichter, A. Nyffeler, M. Passera and P. Stoffer, Phys. Lett. B **735** (2014), 90-91 [arXiv:1403.7512 [hep-ph]].
- [34] S. Komine, T. Moroi and M. Yamaguchi, Phys. Lett. B **506** (2001), 93-98 [arXiv:hep-ph/0102204 [hep-ph]].
- [35] T. Kinoshita and M. Nio, Phys. Rev. D **73** (2006), 053007 [arXiv:hep-ph/0512330 [hep-ph]].
- [36] F. Wang, L. Wu, J. M. Yang and M. Zhang, Phys. Lett. B **759** (2016), 191-199 [arXiv:1512.06715 [hep-ph]].
- [37] B. Allanach, F. S. Queiroz, A. Strumia and S. Sun, Phys. Rev. D **93** (2016) 055045 [erratum: Phys. Rev. D **95** (2017) 119902] [arXiv:1511.07447 [hep-ph]].
- [38] G. Belanger, F. Boudjema, A. Cottrant, R. M. Godbole and A. Semenov, Phys. Lett. B **519** (2001), 93-102 [arXiv:hep-ph/0106275 [hep-ph]].
- [39] D. Chang, W. F. Chang, C. H. Chou and W. Y. Keung, Phys. Rev. D **63** (2001), 091301(R)

[arXiv:hep-ph/0009292 [hep-ph]].

- [40] T. Aoyama, M. Hayakawa, T. Kinoshita and M. Nio, Phys. Rev. Lett. **99** (2007), 110406 [arXiv:0706.3496 [hep-ph]].
- [41] M. Passera, Phys. Rev. D **75** (2007), 013002 [arXiv:hep-ph/0606174 [hep-ph]].
- [42] J. Cao, J. Lian, L. Meng, Y. Yue and P. Zhu, Phys. Rev. D **101**, 095009 (2020) [arXiv:1912.10225 [hep-ph]].
- [43] M. Abdughani, K. I. Hikasa, L. Wu, J. M. Yang and J. Zhao, JHEP **11**, 095 (2019) [arXiv:1909.07792 [hep-ph]].
- [44] F. Wang, K. Wang, J. M. Yang and J. Zhu, JHEP **12**, 041 (2018) [arXiv:1808.10851 [hep-ph]].
- [45] F. Wang, W. Wang and J. M. Yang, Phys. Rev. D **96**, 075025 (2017) [arXiv:1703.10894 [hep-ph]].
- [46] E. Kiritsis and P. Anastopoulos, JHEP **05** (2002), 054 [arXiv:hep-ph/0201295 [hep-ph]].
- [47] B. P. Padley, K. Sinha and K. Wang, Phys. Rev. D **92**, 055025 (2015) [arXiv:1505.05877 [hep-ph]].
- [48] S. P. Li, X. Q. Li and Y. D. Yang, Phys. Rev. D **99**, 035010 (2019) [arXiv:1808.02424 [hep-ph]].
- [49] S. P. Li, X. Q. Li, Y. Y. Li, Y. D. Yang and X. Zhang, JHEP **01**, 034 (2021) [arXiv:2010.02799 [hep-ph]].
- [50] J. Cao, Y. He, J. Lian, D. Zhang and P. Zhu, [arXiv:2102.11355 [hep-ph]].
- [51] N. Chen, B. Wang and C. Y. Yao, [arXiv:2102.05619 [hep-ph]].
- [52] W. Yin, [arXiv:2103.14234 [hep-ph]].
- [53] W. Yin and M. Yamaguchi, [arXiv:2012.03928 [hep-ph]].
- [54] D. Sabatta, A. S. Cornell, A. Goyal, M. Kumar, B. Mellado and X. Ruan, Chin. Phys. C **44**, 063103 (2020) [arXiv:1909.03969 [hep-ph]].
- [55] S. Buddenbrock, A. S. Cornell, Y. Fang, A. Fadol Mohammed, M. Kumar, B. Mellado and K. G. Tomiwa, JHEP **10**, 157 (2019) [arXiv:1901.05300 [hep-ph]].
- [56] S. von Buddenbrock, N. Chakrabarty, A. S. Cornell, D. Kar, M. Kumar, T. Mandal, B. Mellado, B. Mukhopadhyaya, R. G. Reed and X. Ruan, Eur. Phys. J. C **76**, 580 (2016) [arXiv:1606.01674 [hep-ph]].

- [57] N. Okada and H. M. Tran, Phys. Rev. D **94**, 075016 (2016) [arXiv:1606.05329 [hep-ph]].
- [58] T. Fukuyama, N. Okada and H. M. Tran, Phys. Lett. B **767**, 295-302 (2017) [arXiv:1611.08341 [hep-ph]].
- [59] G. Bélanger, J. Da Silva and H. M. Tran, Phys. Rev. D **95**, 115017 (2017) [arXiv:1703.03275 [hep-ph]].
- [60] H. M. Tran and H. T. Nguyen, Phys. Rev. D **99**, 035040 (2019) [arXiv:1812.11757 [hep-ph]].
- [61] E. Chao, Renwick J. Hudspith, Antoine Gerardin, Jeremy R. Green, Harvey B. Meyer, Konstantin Ottnad, arXiv:2104.02632.
- [62] A. E. Carcamo Hernandez, Catalina Espinoza, Juan Carlos Gomez-Izquierdo, Myriam Mondragon, arXiv:2104.02730.
- [63] Andreas Crivellin, Martin Hoferichter, arXiv:2104.03202.
- [64] Motoi Endo, Koichi Hamaguchi, Sho Iwamoto, Teppei Kitahara, arXiv:2104.03217.
- [65] Sho Iwamoto, Tsutomu T. Yanagida, Norimi Yokozaki, arXiv:2104.03223.
- [66] Xiao-Fang Han, Tianjun Li, Hong-Xin Wang, Lei Wang, Yang Zhang, arXiv:2104.03227 .
- [67] Giorgio Arcadi, Lorenzo Calibbi, Marco Fedele, Federico Mescia, arXiv:2104.03228.
- [68] Juan C. Criado, Abdelhak Djouadi, Niko Koivunen, Kristjan Muursepp, Martti Raidal, Hardi Veermae, arXiv:2104.03231.
- [69] Bin Zhu, Xuewen Liu, arXiv:2104.03238.
- [70] Yuchao Gu, Ning Liu, Liangliang Su, Daohan Wang, arXiv:2104.03239.
- [71] Hong-Xin Wang, Lei Wang, Yang Zhang, arXiv:2104.03242.
- [72] Melissa van Beekveld, Wim Beenakker, Marrit Schutten, Jeremy de Wit, arXiv:2104.03245.
- [73] Wen Yin, arXiv:2104.03259.
- [74] Fei Wang, Lei Wu, Yang Xiao, Jin Min Yang, Yang Zhang, arXiv:2104.03262.
- [75] Manuel A. Buen-Abad, JiJi Fan, Matthew Reece, Chen Sun, arXiv:2104.03267.
- [76] Pritam Das, Mrinal Kumar Das, Najimuddin Khan, arXiv:2104.03271.
- [77] Murat Abdughani, Yi-Zhong Fan, Lei Feng, Yue-Lin Sming Tsai, Lei Wu, Qiang Yuan, arXiv:2104.03274.
- [78] Chuan-Hung Chen, Cheng-Wei Chiang, Takaaki Nomura, arXiv:2104.03275.
- [79] Shao-Feng Ge, Xiao-Dong Ma, Pedro Pasquini, arXiv:2104.03276.

- [80] M. Cadeddu, N. Cargioli, F. Dordei, C. Giunti, E. Picciano, arXiv:2104.03280.
- [81] Vedran Brdar, Sudip Jana, Jisuke Kubo, Manfred Lindner, arXiv:2104.03282.
- [82] Junjie Cao, Jingwei Lian, Yusi Pan, Di Zhang, Pengxuan Zhu, arXiv:2104.03284.
- [83] Manimala Chakraborti, Sven Heinemeyer, Ipsita Saha, arXiv:2104.03287.
- [84] Masahiro Ibe, Shin Kobayashi, Yuhei Nakayama, Satoshi Shirai, arXiv:2104.03289.
- [85] Peter Cox, Chengcheng Han, Tsutomu T. Yanagida, arXiv:2104.03290.
- [86] K.S. Babu, Sudip Jana, Manfred Lindner, Vishnu P.K., arXiv:2104.03291.
- [87] Chengcheng Han, arXiv:2104.03292.
- [88] Sven Heinemeyer, Essodjolo Kpatcha, Inaki Lara, Daniel E. Lopez-Fogliani, Carlos Munoz, Natsumi Nagata, arXiv:2104.03294.
- [89] Lorenzo Calibbi, M.L. Lopez-Ibanez, Aurora Melis, Oscar Vives, arXiv:2104.03296.
- [90] D.W.P. Amaral, D.G. Cerdeno, A. Cheek, P. Foldenauer, arXiv:2104.03297.
- [91] Yang Bai, Joshua Berger, arXiv:2104.03301.
- [92] Sebastian Baum, Marcela Carena, Nausheen R. Shah, Carlos E. M. Wagner, arXiv:2104.03302.
- [93] S. Borsanyi, Z. Fodor, J. N. Guenther, C. Hoelbling, S. D. Katz, L. Lellouch, T. Lippert, K. Miura, L. Parato and K. K. Szabo, *et al.* Nature **593**, no.7857, 51-55 (2021).
- [94] D.E. López-Fogliani, C. Muñoz, Phys. Rev. Lett. 97 (2006) 041801, hep-ph/0508297.
- [95] N. Escudero, D.E. López-Fogliani, C. Muñoz, R. Ruiz de Austri, JHEP 12 (2008) 099, arXiv:0810.1507.
- [96] J. Fidalgo, D.E. López-Fogliani, C. Muñoz, R. Ruiz de Austri, JHEP 10 (2011) 020, arXiv:1107.4614.
- [97] P. Bandyopadhyay, P. Ghosh, S. Roy, Phys. Rev. D 84 (2011) 115022, arXiv:1012.5762.
- [98] P. Ghosh, D.E. López-Fogliani, V.A. Mitsou, C. Muñoz, R. Ruiz de Austri, Phys. Rev. D 88 (2013) 015009, arXiv:1211.3177.
- [99] H.-B. Zhang, T.-F. Feng, G.-F. Luo, Z.-F. Ge, S.-M. Zhao, JHEP 07 (2013) 069 [Erratum ibid. 10 (2013) 173], arXiv:1305.4352.
- [100] H.-B. Zhang, T.-F. Feng, S.-M. Zhao, F. Sun, Int. J. Mod. Phys. A 29 (2014) 1450123, arXiv:1407.7365.

- [101] J.E. Kim and H.P. Nilles, Phys. Lett. B 138 (1984) 150.
- [102] H.P. Nilles, Phys. Rep. 110 (1984) 1.
- [103] H.E. Haber, G.L. Kane, Phys. Rept. 117 (1985) 75.
- [104] H.E. Haber, arXiv:hep-ph/9306207.
- [105] S.P. Martin, arXiv:hep-ph/9709356.
- [106] J. Rosiek, Phys. Rev. D 41 (1990) 3464, arXiv:hep-ph/9511250.
- [107] P. Ghosh and S. Roy, JHEP 04 (2009) 069, arXiv:0812.0084.
- [108] A. Bartl, M. Hirsch, S. Liebler, W. Porodc and A. Vicente, JHEP 05 (2009) 120, arXiv:0903.3596.
- [109] J. Fidalgo, D.E. López-Fogliani, C. Muñoz and R.R. de Austri, JHEP 08 (2009) 105, arXiv:0904.3112.
- [110] P. Ghosh, P. Dey, B. Mukhopadhyaya and S. Roy, JHEP 05 (2010) 087, arXiv:1002.2705.
- [111] D.E. López-Fogliani, arXiv:1004.0884.
- [112] H.-B. Zhang, T.-F. Feng, Z.-F. Ge and S.-M. Zhao, JHEP 02 (2014) 012, arXiv:1401.2704.
- [113] H.-B. Zhang, T.-F. Feng, L.-N. Kou and S.-M. Zhao, Int. J. Mod. Phys. A 28 (2013) 1350117, arXiv:1307.6284.
- [114] K.-Y. Choi, D.E. López-Fogliani, C. Muñoz, R.R. de Austri, JCAP 1003 (2010) 028.
- [115] G.A. Gómez-Vargas, M. Fornasa, F. Zandanel, A.J. Cuesta, C. Muñoz, F. Prada, G. Yepes, JCAP 1202 (2012) 001.
- [116] A. Albert et al., JCAP 1410 (2014) 023.
- [117] G.A. Gómez-Vargas, D.E. López-Fogliani, C. Muñoz, A. D. Perez, R.R. de Austri, JCAP 1703 (2017) 047.
- [118] G.A. Gómez-Vargas, D.E. López-Fogliani, C. Muñoz, A.D. Perez, JCAP 01 (2020) 058, arXiv:1911.03191.
- [119] G.A. Gómez-Vargas, D.E. López-Fogliani, C. Muñoz, A.D. Perez, Astropart. Phys. 125 (2021) 102506, arXiv:1911.08550.
- [120] H.-B. Zhang, T.-F. Feng, X.-Y. Yang, S.-M. Zhao, G.-Z. Ning, Phys. Rev. D 95 (2017) 075013, arXiv:1704.03388.
- [121] H.-B. Zhang, T.-F. Feng, F. Sun, K.-S. Sun, J.-B. Chen, and S.-M. Zhao, Phys. Rev. D 89

(2014) 115007, arXiv:1307.3607.

- [122] H.-B. Zhang, T.-F. Feng, S.-M. Zhao, Y.-L. Yan, F. Sun, Chin. Phys. C 4 (2017) 043106, arXiv:1511.08979.
- [123] C.-X. Liu, H.-B. Zhang, J.-L. Yang, S.-M. Zhao, Y.-B. Liu, T.-F. Feng, JHEP 04 (2020) 002, arXiv:2002.04370.
- [124] C.-X. Liu, H.-B. Zhang et al., arXiv:2012.14786.
- [125] D. Hanneke, S. Fogwell and G. Gabrielse, Phys. Rev. Lett. **100**, 120801 (2008).
- [126] R. H. Parker, C. Yu, W. Zhong, B. Estey and H. Muller, Science **360**, 191 (2018).
- [127] L. Morel, Z. Yao, P. Clade, and S. Guellati-Khelifa, Nature 588, 61 (2020).
- [128] P.A. Zyla et al. (Particle Data Group), Prog. Theor. Exp. Phys. 2020 (2020) 083C01, and 2021 update.
- [129] G. Aad et al. [ATLAS Collaboration], Phys. Lett. B 812 (2021) 135980, arXiv:2007.07830.
- [130] A.M. Sirunyan et al. [CMS Collaboration], JHEP 01 (2021) 148, arXiv:2009.04363.
- [131] L. Resnick, M.K. Sundaresan, P.J.S. Watson, Phys. Rev. D 8 (1973) 172.
- [132] J. Ellis, M.K. Gaillard, D.V. Nanopoulos, Nucl. Phys. B 106 (1976) 292.
- [133] D. Y. Bardin, B. M. Vilensky and P. K. Khristova, Sov. J. Nucl. Phys. 53 (1991) 152 [Yad. Fiz. 53 (1991) 240].
- [134] A. Dabelstein, W. Hollik, Z. Phys. C 53 (1992) 507.
- [135] B. A. Kniehl, Nucl. Phys. B 376 (1992) 3.
- [136] B. A. Kniehl, Phys. Rept. 240 (1994) 211.
- [137] A. Djouadi, Phys. Rept. 457 (2008) 1.
- [138] A. Djouadi, Phys. Rept. 459 (2008) 1.
- [139] G. F. Giudice, O. Lebedev, Phys. Lett. B 665 (2008) 79, arXiv:0804.1753.
- [140] N. Vignaroli, Phys. Rev. D 80 (2009) 095023, arXiv:0906.4078.
- [141] A. Dery, A. Efrati, Y. Hochberg, Y. Nir, JHEP 05 (2013) 039, arXiv:1302.3229.
- [142] D. de Florian et al. [LHC Higgs Cross Section Working Group], CYRM-2017-002, arXiv:1610.07922.
- [143] A. Crivellin, D. Mueller, F. Saturnino, arXiv:2008.02643.
- [144] T.F. Feng, X.Y. Yang, Nucl. Phys. B 814 (2009) 101.

- [145] T.F. Feng, L. Sun, X.Y. Yang, Nucl. Phys. B 800 (2008) 221.
- [146] T.F. Feng, L. Sun, X.Y. Yang, Phys. Rev. D 77 (2008) 116008.
- [147] H. Arason, D.J. Castano, B. Keszthelyi, S. Mikaelian, E.J. Piard, P. Ramond and B.D. Wright, Phys. Rev. D 46 (1992) 3945.
- [148] S. Chen et al. (CLEO Collaboration), Phys. Rev. Lett. 87 (2001) 251807.
- [149] A. Limosani et al. (BELLE Collaboration), Phys. Rev. Lett. 103 (2009) 241801.
- [150] T. Saito et al. (BELLE Collaboration), Phys. Rev. D 91 (2015) 052004.
- [151] B. Aubert et al. (BABAR Collaboration), Phys. Rev. D 77 (2008) 051103.
- [152] J. P. Lees et al. (BABAR Collaboration), Phys. Rev. Lett. 109 (2012) 191801.
- [153] J. P. Lees et al. (BABAR Collaboration), Phys. Rev. D 86 (2012) 052012.
- [154] H.-B. Zhang, G.-H. Luo, T.-F. Feng, S.-M. Zhao, T.-J. Gao, K.-S. Sun, Int. J. Mod. Phys. A 29 (2014) 1450196 , arXiv:1409.6837.
- [155] M. Abe et al., Prog. Theor. Exp. Phys. 2019 (2019) 5, 053C02.
- [156] R. Contino et al., CERN Yellow Rep. (2017) no.3, 255-440, CERN-TH-2016-113, arXiv:1606.09408.
- [157] G. Apollinari et al., CERN Yellow Rep. Monogr. 4 (2017) 1-516, CERN-2017-007-M.
- [158] CEPC Study Group, IHEP-CEPC-DR-2018-02, arXiv:1811.10545.
- [159] S. Kawada, J. List, M. Berggren, arXiv:2009.04340.